Noise-induced neural impulses

H. Treutlein and K. Schulten*

Physik-Department, Technische Universität München, D-8046 Garching, Federal Republic of Germany

Abstract. The firing pattern of neural pulses often show the following features: the shapes of individual pulses are nearly identical and frequency independent; the firing frequency can vary over a broad range; the time period between pulses shows a stochastic scatter. This behaviour cannot be understood on the basis of a deterministic non-linear dynamic process, e.g. the Bonhoeffer-van der Pol model. We demonstrate in this paper that a noise term added to the Bonhoeffer-van der Pol model can reproduce the firing patterns of neurons very well. For this purpose we have considered the Fokker-Planck equation corresponding to the stochastic Bonhoeffer-van der Pol model. This equation has been solved by a new Monte Carlo algorithm. We demonstrate that the ensuing distribution functions represent only the global characteristics of the underlying force field: lines of zero slope which attract nearby trajectories prove to be the regions of phase space where the distributions concentrate their amplitude. Since there are two such lines the distributions are bimodal representing repeated fluctuations between two lines of zero slope. Even in cases where the deterministic Bonhoeffer-van der Pol model does not show limit cycle behaviour the stochastic system produces a limit cycle. This cycle can be identified with the firing of neural pulses.

Key words: Nerve cell, nerve impulse, neuronal dynamics, limit cycle, stochastic dynamics

1. Introduction

The coding of information by the electrical activity of nerve cells in the brain is one of the major unsolved problems of science. The relevant electrical activity of nerve cells are action potentials, which travel as spikes along nerve fibres and which are communicated through synapses to other nerve cells. The key to an understanding, of the information code behind neural activity will certainly lie in the aspect that many neurons cooperate in the information processing neural tissues of the brain. However, the signal of *single* neurons as the building block of cooperative neural activity is still of interest.

An important aspect of single nerve cell activity is the frequency of neural pulses travelling along the axon of the nerve cell. This frequency, the firing rate of the neuron, can vary from complete silence, i.e. zero, to about 1 kHz. The shapes of the different pulses in a pulse train elicited by a neuron appear to be mostly identical. On the other hand, the time lag between single pulses in a pulse train scatter statistically around a mean value. This variability in the neuron interspike intervals may be interpreted through two mechanisms which contribute to the dynamics for the generation of pulse trains, a deterministic mechanism (Hodgkin and Huxley 1952) which is responsible for the invariant shape of single pulses and an additional stochastic mechanism (Lecar and Nossal 1971 a, b; Holden 1976; Ricciardi 1982) which does not greatly affect the shape of single pulses, but governs the scatter of the lag time between pulses. An understanding of this latter stochastic mechanism is of obvious interest since this mechanism should also control the average firing rate of neurons in which the information content of the activity of single neurons is encoded.

The deterministic dynamics of single nerve pulses has been described experimentally and theoretically in the celebrated work of Hodgkin and Huxley (Hodgkin and Huxley 1952). These authors established a set of 4-dimensional non-linear differential equations, the so-called Hodgkin-Huxley equations, which account rather well for the shape of nerve pulses of certain neurons, e.g. the squid

---

* To whom offprint requests should be sent

giant axon. The Hodgkin-Huxley equations, in particular, describe the threshold behaviour of pulse generation.

Under the condition that a constant current is applied to the nerve membrane of an axon the Hodgkin-Huxley equations also predict a train of pulses. This pulse train corresponds to a limit cycle solution of the Hodgkin-Huxley equations. The period of this limit cycle and, hence, the lag time between pulses is constant. In this respect the solution differs from the observed behaviour of neurons. In addition, judged by the set of reasonable physiological parameters which enter the Hodgkin-Huxley equations the period of pulse trains can vary only on a small scale: below a certain current (the threshold) the axon after a suitable perturbation exhibits a single pulse and attains a steady-state thereafter. Above the threshold current the axon assumes a limit cycle behaviour the frequency of which varies only by a small margin upon further increase of the membrane current. This behaviour implies that the intrinsic pulse frequency of a neuron can switch only between a value near zero to a constant high value. The Hodgkin-Huxley equations for neurons related to the squid giant axon do not provide a mechanism whereby the firing rate of a neuron could vary continually between zero and a maximum value.

The action potential depends on the behaviour of ion channels in the neural membrane, in particular on the voltage-dependent channel gating. Conduction by single ion channels is inherently noisy, mainly because single channels open and close in a stochastic manner (Koester 1985). However, the accumulative conduction of the large number of ion channels in a neuron's membrane behaves in a rather deterministic manner, as described, for instance, by the Hodgkin-Huxley equations, though one may still expect that the stochastic properties of the single ion channels surface in the macroscopic behaviour of the neural membrane.

The observation (see for example Hennig and Lømo 1985) that recordings from single neurons exhibit a scatter of the lag time between pulses suggested to us that we should model the electrical activity by adding a noise term to the deterministic dynamics. In the following we will show that such a description does, in fact, reproduce the observed firing patterns of neurons: it explains the scatter in the pulse frequency (which is not surprising) and it provides a mechanism for a continuous variation of the pulse frequency from a zero value to a maximum value (which perhaps is surprising).

There exists an abundant literature on the problem addressed above. For example, the connection between single channel properties and the membrane current and membrane potential power spectra was investigated by Conti and Wanke (1975). Much work has been reviewed in the book by Holden (1976). A seminal paper on the subject is that by Lecar and Nossal (1971 a, b). However, all attempts considering stochastic differential equations differ in an important respect from the present investigation. The origin of the difference lies in the difficulty of solving the 4-dimensional system of non-linear differential equations of Hodgkin and Huxley in the presence of noise. In previous investigations, however, the simplifications were carried to an extreme which left the resulting dynamics as being essentially one-dimensional, the case for which textbook solutions are available (Gardiner 1983). This simplification was achieved at the price of model neurons which lack the ability to recover the resting state and can fire only once. In the following we will employ a simplification of a Hodgkin-Huxley neuron in terms of a truly 2-dimensional dynamic system which does not lack this ability. The price we pay is the need for a new numerical method to solve 2-dimensional non-linear stochastic differential equations.

The noise terms assumed in this paper for the dynamics of neural impulses has been described in terms of a most simple process (isotropic additive white noise). In subsequent work one should rather derive the stochastic properties of the noise which acts on the macroscopic action potential from the observed microscopic statistics of single ion channels and of postsynaptic potentials elicited by secondary neurons.

2. Stochastic dynamics of nonlinear systems

2.1. Deterministic dynamics of the Bonhoeffer-van der Pol model

Fitzhugh (1961) has shown that the 4-dimensional dynamics of the Hodgkin-Huxley equations can be projected without much loss of information onto a 2-dimensional manifold. The dynamics in this manifold is described by the equation (Fitzhugh 1961)

$$\partial_t x_1 = c \left(x_1 + x_2 - \tfrac{1}{3} x_1^3 + z \right) = F_1(x), \tag{1a}$$

$$\partial_t x_2 = -\frac{1}{c} \left(x_1 + b x_2 - a \right) = F_2(x). \tag{1b}$$

This equation actually also resulted from the earlier work of Bonhoeffer (1941, 1948, 1953), Bonhoeffer and Langhammer (1948) and van der Pol (1926) and, therefore, is referred to as the Bonhoeffer-van der Pol equation. In Eq. (1), a, b, c, z are external parameters which describe the properties of the neuron. In the following we will adopt the param-

eter values

$$a = 0.7, \quad b = 0.8, \quad c = 3.0 . \tag{2}$$

The parameter z corresponds to the membrane current. This parameter controls the qualitative behaviour of the solution of Eq. (1). This can be demonstrated by means of the eigenvalues of the Jacobian DF of F defined in Eq. (1) which determine the stability of the system near the single stationary point $x_s = (x_{s1}, x_{s2})$ of Eq. (1). For the parameters, (2), the physiologically significant z-range lies between -0.6 and 2.0. One determines that for $z > -0.3465$ the real parts are negative, i.e. the system has a stable focus at x_s. At $z \approx -0.3465$ the real part of $\lambda_{1,2}$ vanishes and the system undergoes a Hopf bifurcation (Guckenheim and Holmes 1983; Marsden and McCracken 1976). At lower values of z one expects that a stable limit cycle exists. This can be shown, in fact, for large c and positive b (Treutlein 1984). Figure 1a and b shows trajectories for the two states, $z = 0$ (a) and $z = -0.4$ (b). In the case of Fig. 1a there exists a stable stationary point and no limit cycle. The trajectories shown all reach the stationary point. In the case of Fig. 1b a stable limit cycle exists and all trajectories converge asymptotically to this limit cycle. It is quite remarkable, however, that although the asymptotic behaviour of the two cases $z = 0$ and $z = -0.4$ is so different the pattern of trajectories is very similar. The reason is that the control parameter z does not affect the global characteristics of the force field $F_1(x)$, $F_2(x)$ of Eq. (1).

The solution of Eq. (1) has been discussed in Treutlein and Schulten (1985). The reader should consult this reference for a better understanding of the present paper.
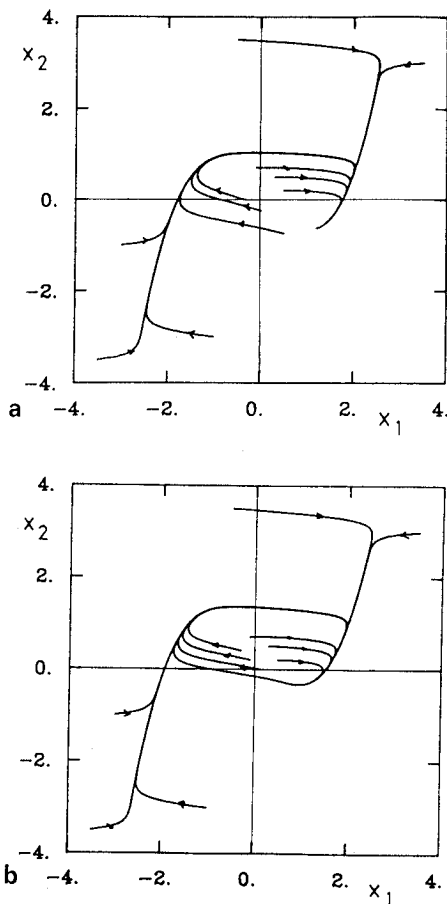

Fig. 1a and b. Sample trajectories of the deterministic Bonhoeffer-van der Pol model as described by Eqs. (2), (2); a for $z = 0$, i.e. a case in which the model does not show limit cycle behaviour and all trajectories end in a stable focus; b for $z = -0.4$, i.e. a case in which the model shows limit cycle behaviour (Treutlein and Schulten 1985)

2.2. Stochastic differential equation and Fokker-Planck equation

In order to model stochastic effects accompanying the dynamics of neural pulse generation we invoke a noise term in the Bonhoeffer-van der Pol equations. For a first exploration of the ensuing stochastic dynamics we choose the simplest realization of noise, namely additive white noise which is isotropic in the x_1- and x_2-directions. The reason for this choice is twofold: (a) For a first exploration on the importance of noise added to the deterministic description of action potentials, the simplest choice should suffice. (b) It is actually not straightforward to derive the statistics of noise acting on a macroscopic level from the microscopic sources mentioned in the Introduction. With the assumed noise the Bonhoeffer-van der Pol equations, (1), are thereby replaced by the stochastic differential equation

$$\partial_t x_1 = F_1(x_1, x_2) + \sigma \, dW_1(t)/dt , \tag{3a}$$

$$\partial_t x_2 = F_2(x_1, x_2) + \sigma \, dW_2(t)/dt , \tag{3b}$$

where $F_i(x)$ are defined as in Eq. (1). This equation differs from the Bonhoeffer-van der Pol equation through the additive noise terms, $\sigma \, dW_i(t)$ represents normalized white noise $[dW_i(t) \, dW_j(t) = \delta_{ij} dt]$ and σ the amplitude of the noise.

The dynamics resulting from the stochastic differential equation, (3), can best be formulated in terms of a distribution function, $p(x, t)$, which describes the probability that an ensemble of systems obeying Eq. (3) is observed with the phase space variables x at time t. This distribution function obeys the following Fokker-Planck equation associated with (3)

$$\partial_t p(x, t) = D \left[\partial_1^2 + \partial_2^2 - \beta \Sigma_i \partial_i F_i(x)\right] p(x, t) \tag{4a}$$

with

$$D = \sigma^2/2 . \tag{4b}$$

$$\beta = 1/D . \tag{4c}$$

By introducing a new timescale $t \to Dt$, Eq. (4a) is transformed to

$$\partial_t p(x, t) = [\partial_1^2 + \partial_2^2 - \beta \Sigma_i \partial_i F_i(x)] p(x, t) . \tag{5}$$

In statistical mechanical applications D corresponds to the diffusion coefficient and β to the inverse temperature. This correspondence implies

large $\beta \leftrightarrow$ weak noise ,

small $\beta \leftrightarrow$ strong noise .

In order to estimate the amplitude of the noise relative to the resting potential, x_{s1}, of the neuron we expand the force $F_1(x)$ around the stationary point x_s. The result is

$$F_1(x_1) = F_1(x_1, x_{2s}) = (x_1 - x_{s1}) c (1 - x_{s1}^2) . \tag{6}$$

Near the stationary point x_s this is linear and one can describe the variation of the potential x_1 under the influence of this force and the noise in Eq. (3a) as a Ornstein-Uhlenbeck process. This yields the stationary distribution

$$p_0(x_1) = [2 \pi \sigma^2]^{-1/2} \exp [-(x_1 - x_{1s})^2/2 \sigma^2] \tag{7a}$$

$$\sigma = [\beta c (x_{s1}^2 - 1)]^{-1/2} . \tag{7b}$$

Here σ describes the RMS variation of the membrane potential. The ratio σ/x_{s1} provides a measure for the observed noise. In the case of a vanishing membrane current, i.e. $z = 0$, one determines

$$\sigma/x_{s1} = 0.7268/\sqrt{\beta} . \tag{7c}$$

For the noise levels β we assume, in the following, values of the order 10 to 100. This implies that the noise measured in units of the resting potential is about 0.1.

2.3. Monte Carlo solution of a 2-dimensional Fokker-Planck equation

The solution of the 2-dimensional Fokker-Planck equation, (5), is a non-trivial task. To obtain the time-dependent distribution and the stationary distribution we will adopt a Monte Carlo algorithm. This algorithm is a generalization of the Brownian dynamics algorithm developed by Lamm and Schulten (1981, 1983).

The key idea of our algorithm is to reduce the time-development of the distribution function into short time steps of duration τ. For this purpose we define the time grid $t_j = j\tau$, $j = 0, 1, 2, \ldots, n$. We consider the conditional probability $p(x, t | x_0, 0)$ to

reach x at time t when the system had assumed the variables x_0 at $t = 0$. By means of the Chapman-Kolmogorov equation one can obtain the representation ($x_n = x$, $t_n = t$)

$$p(x, t | x_0, 0) = \int dx_1 \ldots \int dx_{n-1} \Pi_j p(x_{j+1}, t_{j+1} | x_j, t_j) . \tag{8}$$

Here the conditional probabilities $p(x_{j+1}, t_{j+1} | x_j, t_j)$ represent for $\tau = t_{j+1} - t_j \to 0$ the probabilities for differential displacements.

At this point we take account of the fact that for $\tau \to 0$ the displacements $|x_{j+1} - x_j|$ can be expected to be small. One may, therefore, approximate the force field $F(x)$ *locally around* x_j through the linear expression

$$F_i(x) \approx F_i(x_j) + c_i [x_i - (x_j)_i] \tag{9a}$$

which neglects the off-diagonal linear term and all higher order terms. In this expression

$$b_i = F_i(x_j) \tag{9b}$$

and c_i are constants to be determined locally by a corresponding Taylor expansion of the force field around x_j. This approximation implies

$$p(x_{j+1}, t_{j+1} | x_j, t_j) = \Pi_i \eta_i [(x_{j+1})_i, \tau], \tag{10}$$

where the $\eta_i(x, \tau)$ are solutions of the *local* 1-dimensional Fokker-Planck equation

$$\partial_t \eta_i = \partial_x^2 \eta_i + (c_i x + b_i) \partial_x \eta_i + c_i \eta_i \tag{11a}$$

with initial condition

$$\eta_i(x, 0) = \delta [(x_j)_i] . \tag{11b}$$

The solution of Eq. (11) is the Gaussian

$$\eta_i = (2 \pi \sigma_i^2)^{-1/2} \exp [-(x - \mu_i)^2/2 \sigma_i^2] \tag{12a}$$

$$\sigma_i = [(1 - \theta_i^2)/c_i]^{1/2} \tag{12b}$$

$$\mu_i = (x_j)_i \theta_i - b_i (1 - \theta_i)/c_i \tag{12c}$$

$$\theta_i = \exp(-c_i \tau) . \tag{12d}$$

This Gaussian can be simulated by means of a Monte Carlo procedure invoking a random number W_i corresponding to a standard Gaussian process and setting

$$(x_{j+1})_i = \mu_i + \sigma_i W_i . \tag{13}$$

Equation (8) presents $p(x, t | x_0, 0)$ as a convolution of successive differential displacement distributions, (12), each of which can be simulated as indicated by Eq. (13). Therefore, the Monte Carlo algorithm to evaluate the conditional probability distribution, (8), proceeds as follows: According to Eq. (13) one determines successively by means of standard Gaussian random numbers, W_1 and W_2, the intermediate endpoints $x_0 \to x_1 \to x_2 \to \ldots \to x_n \to$. This calculation simulates the stochastic motion of a

single "particle". In order to obtain the distribution $p(x, t \mid x_0, 0)$ one needs to simulate the motion of a large ensemble of "particles". One then monitors the frequency of the occurrence of endpoints x_j lying within a volume element Δ around a point x of the phase space. This frequency can be identified with

$$p(x, t = j\tau)\Delta.$$

We have found (Treutlein and Schulten 1985) that the stochastic Bonhoeffer-van der Pol model for any initial condition quickly reaches a stationary state. The corresponding stationary distribution can be determined by means of the ensemble average just described, i.e. simulating a large number of trajectories for a long time and monitoring the ensuing endpoint distribution. However, the stationary distribution can be obtained faster by invoking a time average. This can be done by a simulation of a *single* trajectory over a long time recording the frequency with which the endpoints x_j, $j = 0, 1, 2, \ldots$ fall into a volume element Δ of the phase space, e.g. around the point x. This frequency then identifies the stationary distribution, $p(x, t \to \infty)\Delta$.

2.4 Stochastic motion around a limit cycle

The stationary solution of stochastic systems with a deterministic limit cycle $x_L(l)$ for weak and intermediate noise levels is localized around $x_L(l)$. The trajectory $x_L(l)$, $0 \leq l \leq L$ denotes the positions on the limit cycle, the variable l is the length on the limit cycle when the total length is L.

In order to describe the system near the limit cycle we decompose the force field F into two components

$$F \approx F_z + F_p, \tag{14a}$$

where F_z is tangential and F_p is normal to the limit cycle. We assume that we have defined a local coordinate system in which x is represented by a position l on the limit cycle and a coordinate δ measured along the direction n normal to the limit cycle at l, i.e. $x = x_L(l) + \delta n$. For a given x there can exist several such decompositions. This ambiguity, however, should not affect the following considerations. The decomposition (14a) is then chosen as follows

$$F_z = F[x_L(l)] \tag{14b}$$

$$F_p = F - (F \cdot F_z/F_z) F_z/F_z. \tag{14c}$$

(a) Diffusion normal to the limit cycle. The force component (14c) normal to the limit cycle can be represented as

$$F_p(x_L + \delta n) = n \cdot [F(x_L + \delta n) - F(x_L)] n. \tag{15}$$

Taylor expansion yields to 1st order

$$F_p(x_L + \delta n) \approx \alpha(l)\delta n \tag{16a}$$

where

$$\alpha(l) = - n \cdot (n \cdot \nabla F_1, n \cdot \nabla F_2)^T. \tag{16b}$$

This force corresponds to the potential

$$V_p(l, \delta) = \tfrac{1}{2}\alpha(l)\delta^2. \tag{17}$$

The potential, V_p, varies along the limit cycle. It can form a steep well, a flat well or in the case where $\alpha(l) < 0$, a ridge. In the last case one expects stochastic trajectories to diverge from the limit cycle, in the former cases to remain in the neighbourhood of the limit cycle. Only this last case will be considered now.

In the case where the variation of $\alpha(l)$ is not too fast, such that for strong enough noise the distribution adiabatically follows the potential V_p along the limit cycle, and if Eq. (16) is a good approximation to the normal force, one can predict that for $\alpha(l) > 0$

$$p_n(l, \delta) = [\beta\alpha(l)/2\pi]^{1/2} \exp[-\beta\alpha(l)\delta^2/2] \tag{18}$$

describes the variation of the stationary distribution normal to the limit cycle. The amplitude of (18) on the limit cycle is

$$\tilde{p}(l) = [\beta\alpha(l)]^{1/2}. \tag{19}$$

This result shows, in accordance with one's expectations, that for large $\alpha(l)$, i.e. narrow potential wells, the distribution has a large amplitude on the limit cycle whereas for small $\alpha(l)$, i.e. flat potential wells, the amplitude on the limit cycle is small.

(b) Diffusion along the limit cycle. We consider now the stochastic motion along the limit cycle. For this purpose we note that the stochastic differential equation (3) restricted to the limit cycle is

$$\partial_t l = F(l) + \sigma\,dW(t)/dt, \tag{20}$$

where $F(l)$ is the magnitude of the force on the limit cycle. Since the force field $F(x)$ is tangential to the limit cycle we do not require a vectorial representation. The Fokker-Planck equation corresponding to (20) is

$$\partial_t g(l, t) = D[\partial_l^2 - \beta\,\partial_l F(l)]g(l, t) \tag{21a}$$

which has to be solved subject to the cyclic boundary condition

$$g(0, t) = g(L, t), \tag{21b}$$

where L denotes the total length of the limit cycle. $g(l, t)$ describes the amplitude of the distribution along the limit cycle. In the stationary case the fol-

lowing equation holds

$$[\partial_l^2 - \beta \, \partial_l F(l)] \, \tilde{g}(l) = 0 \tag{22a}$$

$$\tilde{g}(0) = \tilde{g}(L). \tag{22b}$$

The solution of this equation is

$$g(l) = C \, e^{-\beta V(l)} \, [\int_0^l e^{\beta V(l')} \, dl' \\ + (e^{\beta V(l)} - 1)^{-1} \int_0^L e^{\beta V(l')} \, dl'], \tag{23a}$$

where C is a normalization constant and

$$V(l) = -\int_0^l F(l') \, dl'. \tag{23b}$$

This solution satisfies the cyclic boundary condition (22b). Since the conditions $F(0) = F(L)$ and

$$\partial_l g(l) = F(l) \, g(l) + C$$

hold, (23) has also a continuous derivative at $l = 0$.

In general, the numerical evaluation of $g(l)$ according to (23) requires a very high numerical precision as can be shown by a test of the cyclic boundary condition. However, it is often sufficient to consider the limiting cases of weak and strong noise. In the case of weak noise the following equation holds, instead of (22a)

$$\partial_l F(l) \, g(l) = 0 \tag{24a}$$

and, hence,

$$g(l) = C'/F(l) \tag{24b}$$

for some constant C'. In the case of strong noise, i.e. small β, the following equation holds instead of (22a)

$$\partial_l^2 g(l) = 0 \tag{25a}$$

and, hence, $g(l)$ should be constant

$$g(l) = C''. \tag{25b}$$

As a demonstration of a stochastic motion along a limit cycle we consider the following force field:

$$F(x) = F_p(x) + F_z(x) \tag{26a}$$

$$F_p(x) = -\nabla U(x) \tag{26b}$$

$$U(x) = [a(x_1^2 + x_2^2 - l^2)] \tag{26c}$$

$$F_z(x) = c(x)(x_1, -x_1)^T \tag{26d}$$

$$c(x) = b[\cos(4\varphi) + 1] \tag{26e}$$

$$\tan \varphi = x_1/x_2. \tag{26f}$$

The resulting force field induces a limit cycle along the circle $x_1^2 + x_2^2 = l^2$. It can easily be shown, that $F_p \cdot F_z = 0$. A constant function $c(x) = c$ would yield a stationary distribution function of the form

$$p(x, t \to \infty) \propto \exp(-\beta U(x)), \tag{27}$$

because of $\nabla \cdot F_z = 0$ (Treutlein 1984). However, since in (26e) $\nabla \cdot F_z \neq 0$ the stationary distribution differes from (27). The distribution for the two choices of noise levels ($\beta = 1, 10$) is shown in Fig. 2a

and b. The spatial dependence of $c(x)$ induces four maxima. Figure 2c and d presents the distribution along the limit cycle. The force normal to the circular limit cycle is radial symmetric and, hence, the diffusion normal to the limit cycle is independent of the azimuthal angle φ. As a result the distribution along the limit cycle is solely determined by the stochastic motion along the limit cycle and, therefore, described by Eq. (22) in the stationary case. As shown for the two noise levels $\beta = 0.5, 6$ in Fig. 2c and d a comparison of the Monte Carlo simulation with the distribution predicted by Eq. (23) is satisfactory. These figures demonstrate two effects of the noise level on the limit cycle diffusion: (i) large noise diminishes the variation of the distribution along the limit cycle such that for very large noise levels the distribution becomes constant; (ii) an increase of the noise level from small to large values induces a shift of the distribution maxima from the force minima to the force maxima.

(c) Summary. The following conclusions for an approximate analytical description of the stationary distribution function with stochastic limit cycle behaviour can be drawn. The distribution near the limit cycle is affected by two stochastic processes, namely (i) normal, (ii) tangential to the limit cycle, which are often approximately independent. For strong noise the tangential diffusion leads to a constant distribution and, hence, does not influence the total distribution. The normal diffusion induces a distribution amplitude on the limit cycle according to (19). Therefore, the total distribution should behave as

$$p_{\text{appr}}(l) = \tilde{p}(l). \tag{28}$$

In the case of weak noise the diffusion normal to the limit cycle does not follow adiabatically the limit cycle, i.e. the variation of $\alpha(l)$ as given by (16b). One may, hence, assume $\tilde{p}(l) = \text{const.}$ and neglect the normal diffusion. The contribution of the tangential diffusion in the limit of weak noise is given by (24b) and, therefore, the total distribution should behave as

$$p_{\text{appr}}(l) = C'/F(l), \tag{29}$$

where F is the magnitude of the force on the limit cycle.

3. Stochastic dynamics of neural pulses/Results

3.1 Deterministic limit cycle with noise

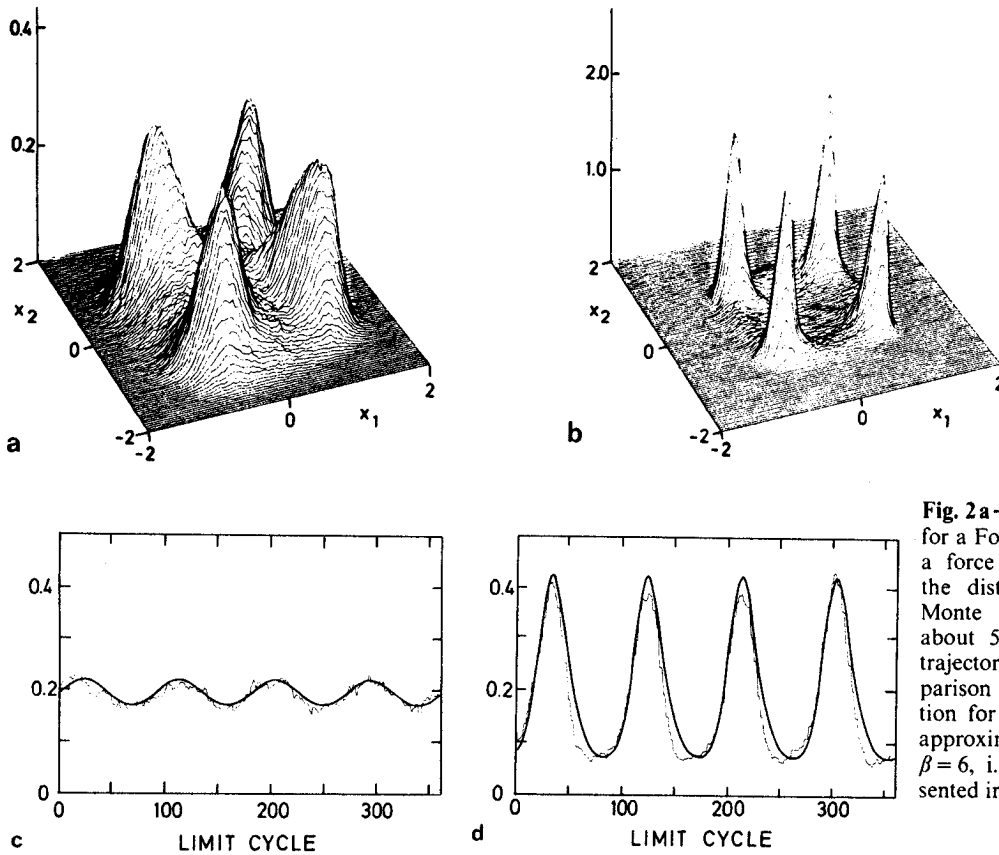Employing the Monte Carlo method outlined in Sect. 2.3 we have determined (Treutlein and Schulten

Fig. 2a–d. Stationary distribution for a Fokker-Planck system, (3), and a force field, (26), with $b = l = 1$; the distributions resulted from a Monte Carlo simulation sampling about 5 000 000 points of a single trajectory; **a** $\beta = 6$; **b** $\beta = 60$; **c** comparison of a Monte Carlo distribution for $\beta = 0.5$ with the analytical approximation (23); **d** same as **c** for $\beta = 6$, i.e. for the distribution presented in **a**

1985) the time-dependent distribution for the stochastic Bonhoeffer-van der Pol model, (5), in the case where $z = -0.4$, i.e. when the deterministic Eq. (1) yields a stable limit cycle. The results showed that the system very quickly reaches a stationary distribution. Hence, it appears sufficient to characterize the Bonhoeffer-van der Pol model by its stationary distribution. For this purpose we present in Fig. 3 this distribution for a noise level $\beta = 10$. The distribution is mainly concentrated around the limit cycle observed for the deterministic system. The distribution along the limit cycle is, however, distinctly bimodal. The maximum values of the distribution are situated along the two local attractors which characterize the Bonhoeffer-van der Pol model (Treutlein and Schulten 1985). The bimodal distribution can be rationalized by noting that the force $F(l)$ along the deterministic limit cycle assumes two minimum values on the two local attractors, i.e. the distribution along the limit cycle should assume two maxima on the two attractors.

3.2 Noise-induced limit cycle behaviour

We want to consider now the stochastic Bonhoeffer-van der Pol model in the case of zero membrane current, i.e. $z = 0$. For this z value the deterministic
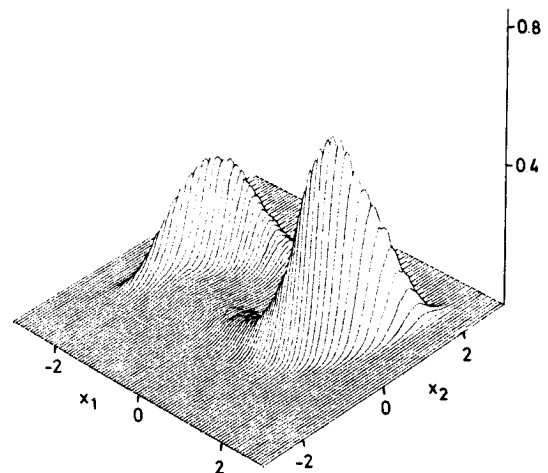

Fig. 3. Stationary distribution of the stochastic Bonhoeffer-van der Pol model with $z = -0.4$ for the noise level $\beta = 10$; the distributions resulted from single Monte Carlo trajectories sampling about 29 000 000 points (Treutlein and Schulten (1985)

model does not show a limit cycle behaviour but rather approaches a stable focus. Figure 4a and b show the stationary distribution of the stochastic system for the two noise levels $\beta = 10$ and $\beta = 100$. A comparison of the distributions of Figs. 3 and 4a which both correspond to $\beta = 10$ but to different z
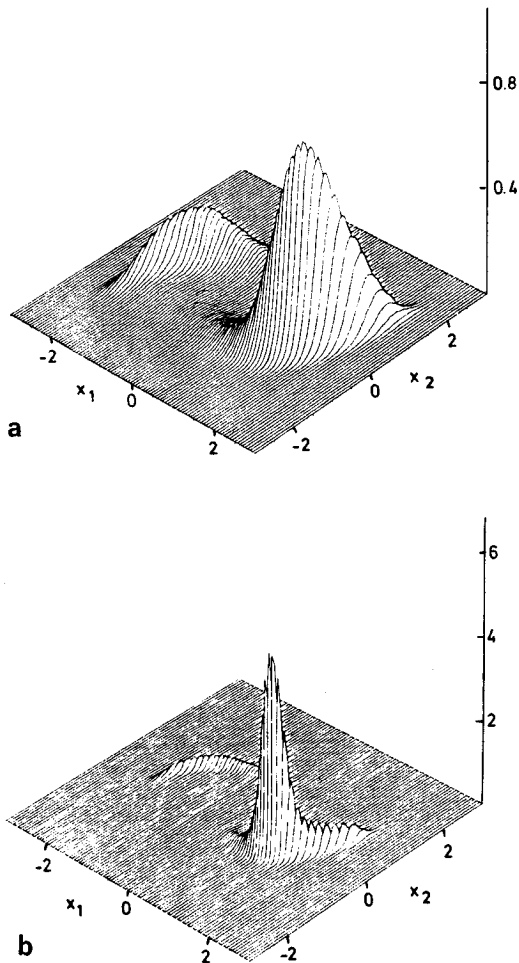
Fig. 4 a and b. Stationary distribution of the stochastic Bonhoeffer-van der Pol model for $z = 0$, i.e. the case that no deterministic limit cycle exists; the distributions results from a Monte Carlo trajectory sampling about 29 000 000 jump points; **a** $\beta = 10$, **b** $\beta = 100$ (Treutlein and Schulten 1985)
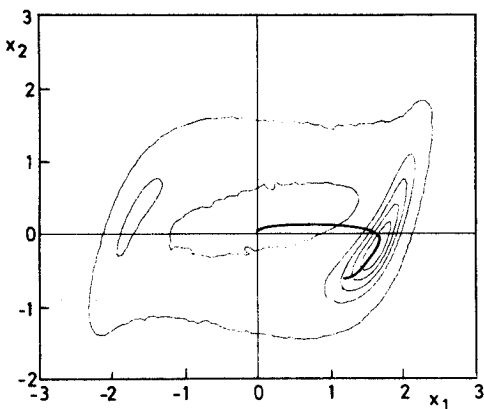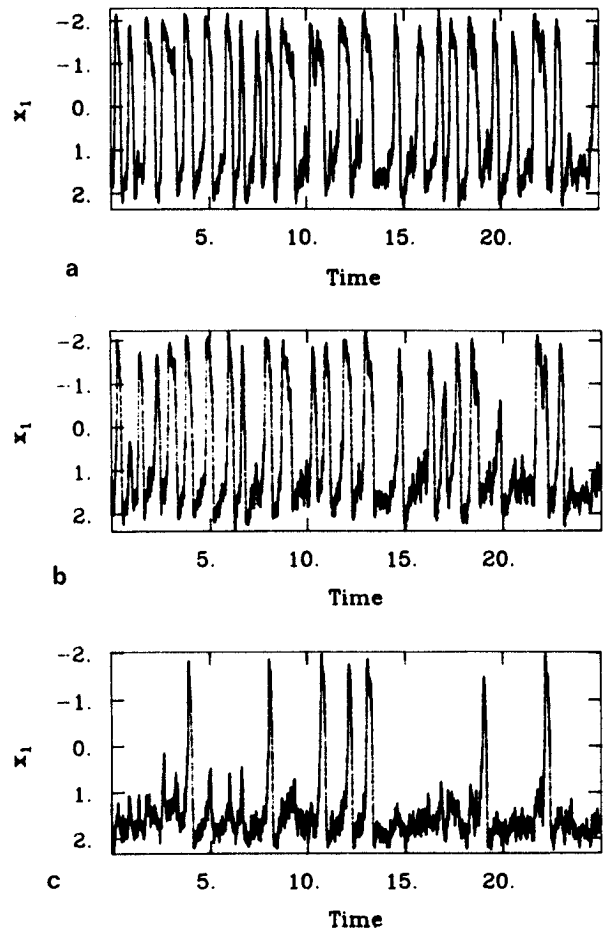

Fig. 6 a – c. Trace of the x_1 variable of a Monte Carlo trajectory for the stochastic Bonhoeffer-van der Pol model with $\beta = 10$ representing the electrical membrane potential of a neuron; **a** $z = -0.4$ (limit cycle situation), **b** $z = 0$ (no limit cycle), **c** $z = 1$ (no limit cycle)

Fig. 5. Contour plot representation of the distribution in Fig. 4a superimposed on a deterministic trajectory (Treutlein and Schulten 1985)

values, namely $z = -0.4$ and $z = 0$, respectively, shows that the stochastic system for $z = 0$ behaves almost identically to the $z = -0.4$ limit cycle system. The difference in the behaviour between the stochastic system and the deterministic system is demonstrated in Fig. 5 which presents the contour lines to Fig. 4a superimposed on a deterministic trajectory. This trajectory approaches most directly the stable focus. In contrast the stochastic system exhibits a bimodal distribution which represents repeated jumps of stochastic trajectories between the two local attractors. Even in the case of weak noise the distribution is bimodal as seen in Fig. 4b. The interpretation of this finding is that the noise induces the Bonhoeffer-van der Pol model to move along the limit cycle in a parameter range where the deterministic system does no show limit cycle behaviour.
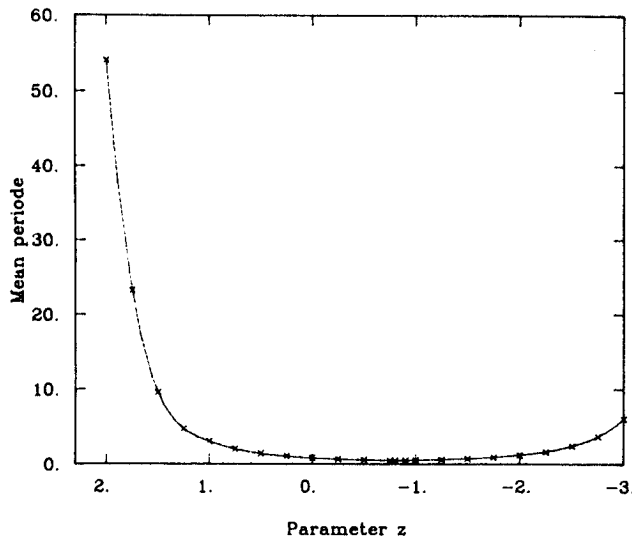
Fig. 7. Dependence on the current z of the mean period between neural pulses for the stochastic Bonhoeffer-van der Pol model as described by Monte Carlo simulations (constant noise level $\beta = 10$)
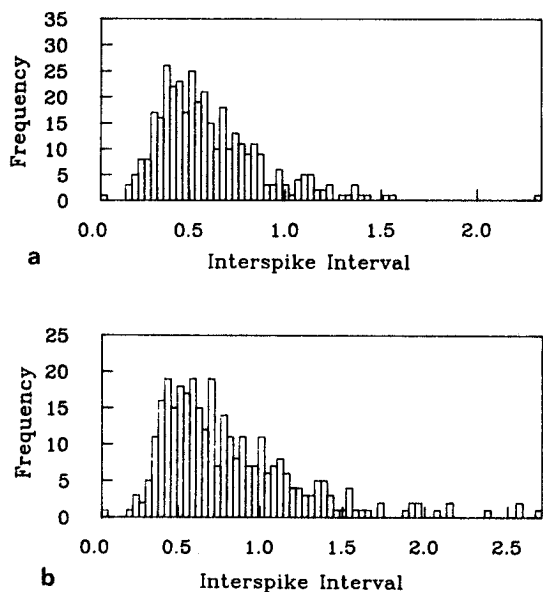

a

b

Fig. 8a and b. Distribution of interspike intervals for the stochastic BvP model with $\beta = 10$ and **a** $z = -0.5$ (**b**) $z = 0$

3.3 Variation of the firing rate of neural pulses

We finally consider the problem posed in the Introduction, namely how neurons vary the firing rate of the nerve pulses. Figures 6a–c show time traces of the x_1 variable of the stochastic Bonhoeffer-van der Pol model for $z = -0.4$ (a), $z = 0$ (b), and $z = 1.0$ (c) i.e. the cases in which the deterministic system does (a) and does not (b), (c) show a limit cycle. The traces of x_1 are remarkably similar to physiological recordings of single nerve cells in that the shapes of single pulses are rather invariant
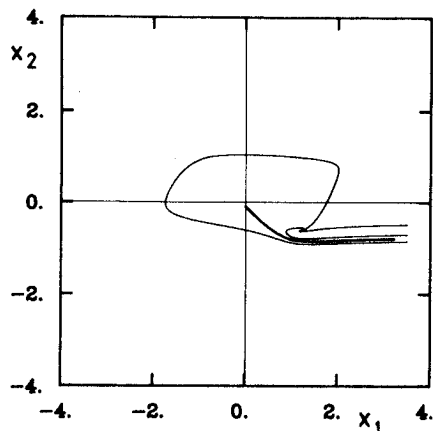

Fig. 9. Sample trajectories approaching the stable focus and sparatrix line (see text) for the Bonhoeffer-van der Pol model with $z = 0$ (Treutlein and Schulten 1985)

but a scatter in the time between pulses is observed. The recording of the system in Fig. 6b corresponds to the distribution in Fig. 4a. Every pulse corresponds to a round along a noise-induced limit cycle.

The question of how the frequency of pulses varies when the membrane current z is changed is addressed in the diagram of Fig. 7. This figure shows for the case $\beta = 10$ how the mean period between pulses depends on z. Altering z from about -1.0 to about $+2.0$ induces a 55-fold increase of the mean time between pulses. Further variation of z increases the time even further such that the pulse frequency can virtually be varied continuously from zero to a high value. On the basis of this result we like to suggest then that neurons, in order to code the frequency of their axonic pulses, either employ intrinsic electrical membrane noise or use for that purpose the electrical signals of synapses converging on them (which most likely appear like noise). This result corresponds to a similar finding of Lecar and Nossal (1971 a).

The distribution of interspike intervals is shown in Fig. 8a and b for the parameters $\beta = 10$ and $z = -0.5$ (a) and $z = 0$ (b). This result compares qualitatively to a recent observation of the frequency distribution of interspike intervals of motor units in rats (Hennig and Lømo 1985).

We wish to comment finally on the mechanism which controls the noise-induced pulse generation in the framework of the Bonhoeffer-van der Pol model. This mechanism can be explained by means of Fig. 9. This figure shows the stationary point from which all stochastic trajectories start. For the membrane currents $z < -0.35$ considered here the stationary point is stable for the deterministic system. However, stochastic trajectories succeed in crossing the local separatrix determined by us recently (Treutlein and Schulten 1985) and then produce a
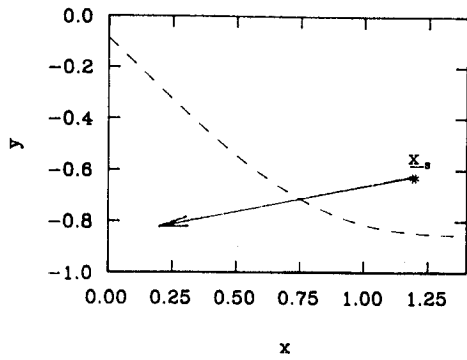
Fig. 10. Integration path for the potential energy according Eq. (30). The dashed line represents the separatrix (see Fig. 9)
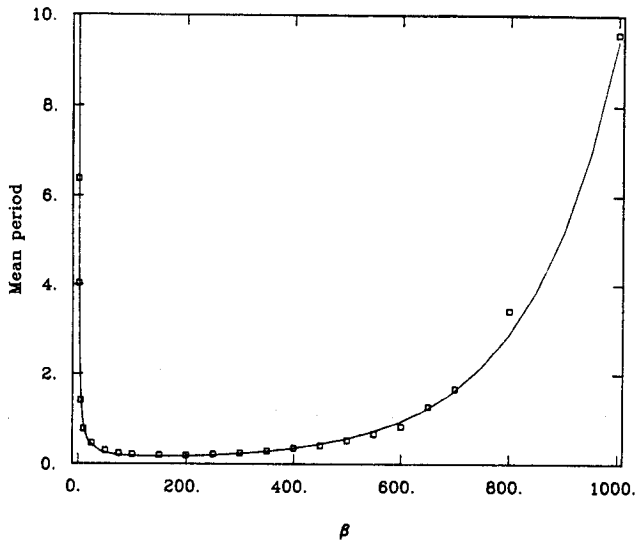

Fig. 11. Dependence on the noise level β of the mean period between neural pulses for the stochastic Bonhoeffer-van der Pol model as described by Monte Carlo simulations. The solid line shows the result of the Kramer's theory, i.e. Eq. (31), the squares represent the data obtained from the simulation ($z = 0$). In applying (31) we have choosen the line segment in Fig. 10.

neural spike since on the left of the sparatrix a recovery of the resting state is possible only by a detour which assumes low intermediate potential values. The frequency of stochastically induced neural spikes can be reproduced quantitatively if one assumes the stochastic motion of the system along the line indicated in Fig. 10. The ensuing motion is 1-dimensional and, hence, a potential $U(x)$ can be defined when x is the distance from the stationary point x_s

$$U(x) = - \int_0^x dx' \cdot F(x') \tag{30}$$

$U(x)$ assumes a minimum at $x = 0$ and a maximum at a value $x = x_m$. Applying Kramer's theory for barrier crossing (Risken 1985) yields an expression

for the mean time lag $\langle \tau \rangle$ between two pulses:

$$\langle \tau \rangle = (\alpha/\beta) \exp(\beta \, \Delta U) \tag{31}$$

with

$$\Delta U = U(x_m) \tag{32}$$

and

$$\alpha = 2 \pi / \{\partial_x^2 U(0) \, \partial_x^2 U(x_m)\}^{1/2} . \tag{33}$$

In applying formulas (31)−(33) the reader should note that the physical mean time lag is actually $\langle \tau \rangle / D$ [see below Eq. (4)]. Figure 11 compares, for $z = 0$, $\langle \tau \rangle$ evaluated according to Eq. (31) with the $\langle \tau \rangle$ values obtained from a simulation of stochastic trajectories. This comparision shows that the approximation (31) reproduces the exact τ values over a wide range of β values. We consider the simple analytical approximation (31) an important result of this paper as it relates the stochastic aspects of excitability entailed in β and D to the macroscopic behaviour of neural impulses as described by $\langle \tau \rangle$.

References

Bonhoeffer KF (1941) Über die Aktivierung von passiven Eisen in Salpetersäure. Z Elektrochem 47:147

Bonhoeffer KF (1948) Activation of passiv iron as a model for the excitation of nerve. J Gen Physiol 32:69

Bonhoeffer KF (1953) Modelle der Nervenerregung. Naturwissenschaften 40:301

Bonhoeffer KF, Langhammer G (1948) Über periodische Reaktionen. IV. Theorie der kathodischen Polarisation von Eisen in Salpetersäure. Z Elektrochem 52:67

Conti F, Wanke E (1975) Channel noise in nerve membranes and lipid bilayers. Qu Rev Biophys 8(4):451

Fitzhugh R (1961) Impulses and physiological states in theoretical models of nerve membranes. Biophys J 1:445

Gardiner CW (1983) Handbook of stochastic methods for physics, chemistry and the natural sciences. Springer, Berlin Heidelberg New York (Springer Series in Synergetics, vol 13)

Guckenheim J, Holmes P (1983) Nonlinear oszillations, dynamical systems, and bifurcation of vector fields. Springer, Berlin Heidelberg New York (Appl Math Sci, vol 42)

Hennig R, Lømo T (1985) Firing patterns of motor units in normal rats. Nature 314:164

Holden AV (1976) Models of the stochastic activity of neurons. Springer, Berlin Heidelberg New York (Lecture Notes in Biomathematics, vol 12)

Hodgkin AL, Huxley AF (1952) A quantitative description of membrane current and its application to conduction and excitation in nerve. J Physiol 117:500

Koester J (1985) Voltage-gated Channels and the generation of the action potential. In: Kandel ER, Schwartz JH (eds) Principles of neural science. Elsevier, New York Amsterdam Oxford

Lamm G, Schulten K (1981) Extended Brownian dynamics approach to diffusion-controlled processes. J Chem Phys 75:365

Lamm G, Schulten K (1983) Extended Brownian dynamics. II. Reactive, nonlinear diffusion. J Chem Phys 78:2713

Lecar H, Nossal R (1971a) Theory of threshold fluctuations in nerves. I. Biophys J 11:1048

Lecar H, Nossal R (1971b) Theory of threshold fluctuations in nerves. II. Biophys J 11:1068

Marsden J, McCracken M (1976) The Hopf-bifurcation and its applications. Springer, Berlin Heidelberg New York (Appl Math Sci, vol 19)

Ricciardi LM (1982) Diffusion approximations and computational problems for single neutrons' activity. In: Levin S (ed) Competition and cooperation in neural nets. Springer, Berlin Heidelberg New York (Lecture Notes in Biomathematics, vol 45)

Risken H (1985) The Fokker-Planck equation; methods of solution and applications. Springer, Berlin Heidelberg New York (Springer series in Synergetics, vol 18)

Treutlein H (1984) Die Lösungen der Fokker-Planck Gleichung zur Beschreibung nicht-linearer Reaktionen mit additivem Rauschen. Diplomarbeit, Technische Universität München

Treutlein H, Schulten K (1985) Noise induced limit cycles of the Bonhoeffer-van der Pol model of neural pulses. Ber Bunsenges Phys Chem 89:710

van der Pol B (1926) On relaxation oscillations. Philos Mag 2:978